

# Magnetic parameters and rotational mobility of the $\equiv\text{SiON}(\text{O}^\cdot)\text{CX}_3$ nitroxides (X = H, D) grafted on silica surface

V. I. Pergushov,\* T. A. Klimenko, D. A. Tyurin, and A. Kh. Vorob'ev

Department of Chemistry, M. V. Lomonosov Moscow State University,  
Leninskie Gory, 119899 Moscow, Russian Federation.  
Fax: +7 (095) 932 8846. E-mail: pvi@excite.chem.msu.su

The magnetic parameters of the  $\equiv\text{SiON}(\text{O}^\cdot)\text{CX}_3$  nitroxides (X = H, D) grafted on an activated Aerosil surface were determined. The optimal geometry of the radicals was calculated and their rotational mobility was characterized. The activation energies to the rotation of radical fragments around various bonds were estimated.

**Key words:** grafted nitroxides, magnetic parameters, rotational mobility of radicals, activation energy to the rotation of radical fragments, silica.

Studies of nitroxides have resulted in considerable progress in the development of the theory of structure of organic radicals, molecular and conformational dynamics of species, and intermolecular interactions.<sup>1–5</sup> Investigation of the dynamics of radicals either grafted or adsorbed on the surface of a solid support can provide structural information on the local environment of a paramagnetic species.<sup>6</sup> Preparation of grafted nitroxides with the paramagnetic fragments located in the close vicinity of the solid surface and the possibility of using them as peculiar spin probes have been reported previously.<sup>7</sup> In this study, the magnetic-resonance parameters and the structural characteristics of these probes were determined, the conformations of grafted nitroxides were established, and their rotational mobility was studied.

## Experimental

The  $\equiv\text{SiON}(\text{O}^\cdot)\text{CX}_3$  nitroxides were prepared by the reaction of the  $\text{CX}_3\text{NO}_2$  vapor (X = H, D) with tricoordinate silicon atoms  $\equiv\text{Si}^\cdot$  stabilized on the thermochemically activated silica surface (Aerosil A-175); the procedure for thermochemical activation of the Aerosil surface was described previously.<sup>8</sup>

ESR spectra were recorded on an E-3 radiospectrometer (Varian). The sample temperatures of  $>77$  K were maintained using a cryostat, in which a stream of nitrogen (vaporized from a Dewar vessel) having a specified temperature was blown through a tube placed directly in the cavity of the ESR spectrometer. The temperature was maintained automatically using an E-4557-9 standard attachment (accuracy  $\pm 1^\circ$ ). The reference points used in the determination of isotropic *g*-factors were the effective values of *g*-factors of the third and fourth HFS components for diamagnetically diluted  $\text{Mn}^{2+}$  ions in  $\text{MgO}$  ( $g_3 = 2.0328 \pm 0.0001$ ,  $g_4 = 1.9812 \pm 0.0001$ ), the distance between them, equal to  $86.76 \pm 0.05$  G at  $20^\circ\text{C}$  (data of All-Union Institute Of Physico-Technical and Radio Measurements), and the known<sup>9</sup> value  $g_\perp = 2.00055$  for the  $\equiv\text{Si}^\cdot$

radical. The *g*-tensor components of the radicals were determined during the simulation of the ESR spectra with a fixed isotopic *g*-factor.

The ESR spectra of nitroxides were simulated with the assumption that no averaging of the anisotropic Zeeman and hyperfine couplings takes place (rigid limit assumption) using a program developed previously by an author of this communication (A. Kh. Vorob'ev). The simulation of the ESR spectra with allowance for the rotational mobility of radicals was performed using a slightly modified program (version 1.6),<sup>10</sup> which permits the calculation of anisotropic ESR spectra of nonrigidly fixed radicals with hyperfine structure due to one nucleus. The optimal values of parameters for the description of experimental ESR spectra were found by the nonlinear least-squares method with variation of the variable parameters. The deviations of the simulated spectra from experimental ones were minimized by an adaptive procedure.<sup>11</sup>

In the rigid limit simulation of ESR spectra, the minimum was found by varying the magnetic parameters of radicals (components of the *g*-tensor and the HFC tensors, the angles between them, and the half-widths of the individual spectral lines); the *g*-tensor components and the HFC constants estimated from the experimental spectra were taken as the initial values.

The rotational mobility of the grafted radicals was analyzed using the ESR spectra recorded at 120–180 K. In the simulation, only values characterizing the dynamic behavior of the species were varied (components of the rotational diffusion tensor **R**, the angles between the *g* and **R** tensor components, and the half-width of individual lines); the magnetic parameters calculated by the rigid limit procedure were maintained constant. The simulation was considered satisfactory if the positions of the maxima of the simulated and experimental spectra coincided and the sum of squared deviations of the simulated spectra from the experimental one was approximately equal to the sum of squared deviations caused by noises in the experimental spectrum. The procedures for the rigid limit simulation of the ESR spectra of rotating radicals were described in more detail previously.<sup>12</sup>

The density functional technique (DFT) quantum-chemical calculations were performed using an original program developed and kindly provided by D. N. Laikov.<sup>13</sup>

## Results and Discussion

**Magnetic-resonance parameters and conformations of radicals.** The pattern of the experimental ESR spectra of the grafted  $\equiv\text{SiON}(\text{O}^\cdot)\text{CX}_3$  radicals ( $X = \text{H}, \text{D}$ ) at 77 K points to anisotropy of the  $\mathbf{g}$ -tensor and anisotropy of the tensors of HFC (tensors  $\mathbf{A}$ ) with all magnetic nuclei in these radicals (Fig. 1, *a*, *b*, curves 1). The

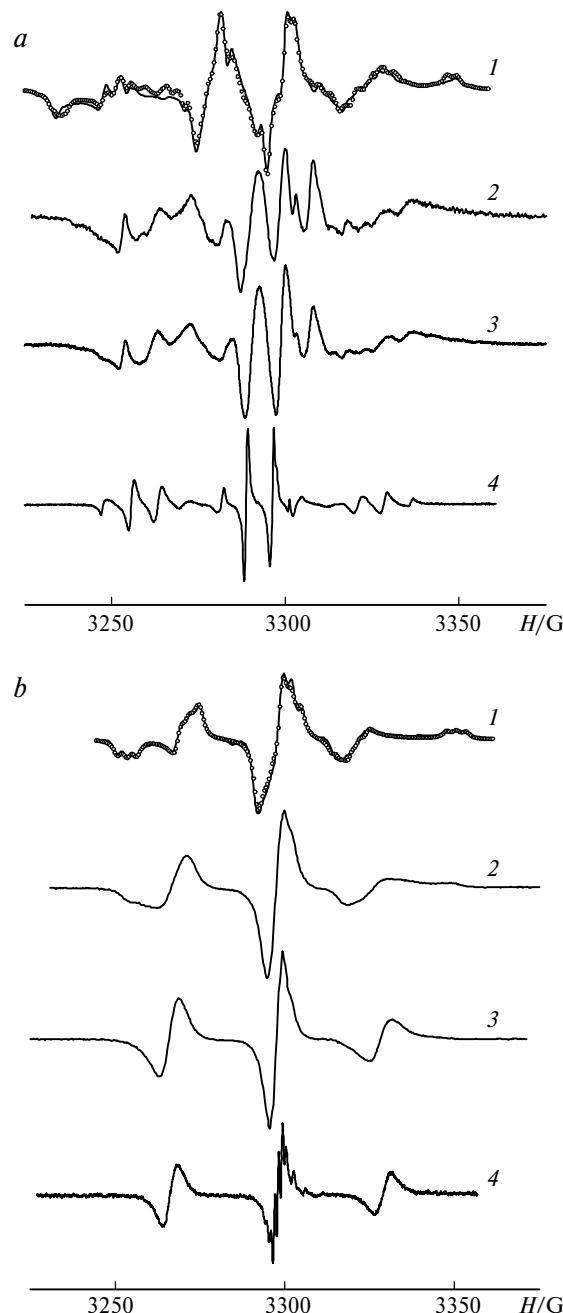


**Fig. 1.** ESR spectra of the  $\equiv\text{SiON}(\text{O}^\cdot)\text{Me}$  (*a*) and  $\equiv\text{SiON}(\text{O}^\cdot)\text{CD}_3$  (*b*) radicals at 77 (1), 120 (2), 180 (3), and 298 K (4). The continuous lines show experimental spectra and the dots correspond to calculations.

**Table 1.** Magnetic-resonance and structural parameters of grafted radicals

| Radical  | Com- | $g$    | $\mathbf{A}^a/\text{G}$ |                    |                    |                    |  |
|--|------|--------|-------------------------|--------------------|--------------------|--------------------|--|
|  |      |        | $\mathbf{N}^b$          | H(1)<br>or<br>D(1) | H(2)<br>or<br>D(2) | H(3)<br>or<br>D(3) |  |
| $\equiv\text{SiON}(\text{O}^\cdot)\text{Me}$   | $xx$ | 2.0059 | 27.4 (21.5)             | 12.6               | 8.8                | 5.6                |  |
|  | $yy$ | 2.0067 | 20.2 (21.2)             | 19.9               | 1.0                | 1.6                |  |
|  | $zz$ | 2.0026 | 47.1 (46.9)             | 20.7               | 2.3                | — <sup>c</sup>     |  |
| $\equiv\text{SiON}(\text{O}^\cdot)\text{CD}_3$ | $xx$ | 2.0059 | 25.4                    | 2.5                | — <sup>c</sup>     | — <sup>c</sup>     |  |
|  | $yy$ | 2.0070 | 21.9                    | 2.6                | — <sup>c</sup>     | — <sup>c</sup>     |  |
|  | $zz$ | 2.0023 | 48.6                    | 2.9                | — <sup>c</sup>     | — <sup>c</sup>     |  |

<sup>a</sup> HFC tensor with magnetic nuclei.

<sup>b</sup> The values in parentheses are the calculated values for the HFC tensor components.

<sup>c</sup> The corresponding values have not been determined reliably.

theoretical spectra simulated under the rigid limit assumption are in good agreement with experimental ones. The calculated components of the  $\mathbf{g}$  and  $\mathbf{A}$  tensors (the accuracies of determination of the parameters are estimated to be  $\sim 0.0001$  and  $\sim 0.1$  G, respectively) are presented in Table 1. The  $\mathbf{g}$ -tensor and HFC tensor components (see Table 1) were assigned on the basis of joint analysis of the results given in Table 1 and the data on rotational mobility of radicals, which will be considered below. The  $x$ -component of the  $\mathbf{g}$ -tensor found for the grafted radical is smaller than the  $y$ -component, whereas for known nitroxides of various structures,  $g_{xx} > g_{yy}$ .<sup>1,3,5,14</sup> Meanwhile, the  $g_{zz}$  values determined for grafted radicals are in good agreement with analogous values for nitroxides. In our opinion, this relationship ( $g_{xx} < g_{yy}$ ) found for the grafted radical is due to the possibility of conjugation of the unpaired electron with the  $n$ -electrons of the O atom of one of the substituents at the N atom ( $\equiv\text{Si}—\text{O}—$ ). Previously,<sup>14</sup> analysis of an array of experimental data obtained by ESR in the Q-range for 68 nitroxides of various structures demonstrated the trend of the  $g_{xx}$  values to decrease with enhancement of the interaction between the  $\pi^*$  orbital of the N—O<sup>·</sup> bond and the  $\pi$ -type orbitals concentrated at the periphery of the radical, although the inequality  $g_{xx} > g_{yy}$  held for all radicals. To date, there are no arguments at our disposal for substantiated discussion of this topic.

The optimal geometry (Table 2) and the isotropic HFC constants for the N and H nuclei in the  $\text{F}_3\text{SiON}(\text{O}^\cdot)\text{Me}$  radical were found by DFT calculations (Table 3); the tricoordinate Si atom on the silica surface was described using the  $\text{SiF}_3$  fragment<sup>15</sup> or the  $\text{Si}_4\text{O}_9\text{H}_3$  cluster. The two calculation procedures gave similar results.

The obtained geometric parameters (see Table 2) are in reasonable agreement with known experimental data; in the di-*tert*-butylnitroxyl, the N—O<sup>·</sup> and C—N bond lengths are 1.28 and 1.51 Å, respectively and the angle

**Table 2.** Bond lengths ( $d$ ) and planar ( $\omega$ ) and dihedral ( $\tau$ ) angles characterizing the optimal geometry of the  $F_3SiON(O^\cdot)Me$  radical

| Parameter          | Value               |
|--------------------|---------------------|
| Bond               | $d/\text{\AA}$      |
| N—O $^\cdot$       | 1.24                |
| C—N                | 1.47                |
| N—O                | 1.52                |
| Si—O               | 1.66                |
| The planar angle   | $\omega/\text{deg}$ |
| $\varphi^*$        | 42.8                |
| C—N—O              | 106                 |
| O—N—O $^\cdot$     | 117                 |
| Si—O—N             | 115                 |
| The dihedral angle | $\tau/\text{deg}$   |
| Si—O—N—C           | 163                 |
| Si—O—N—O $^\cdot$  | 24                  |
| O—N—C—H(1)         | 70                  |
| O—N—C—H(2)         | -173                |

\* The angle between the C—N—O plane and the N—O $^\cdot$  bond.

$\varphi \approx 0^\circ$ ,<sup>16</sup> the Si—O bond lengths in most organic compounds are in the range of  $1.64 \pm 0.03 \text{ \AA}$ .<sup>17</sup> The calculated values of the HFC tensor with the N nuclei (isotropic constant  $A_{\text{iso}} \approx 29.9 \text{ G}$ ; the anisotropic components of the HFC with the N atom:  $B_{xx} \approx -8.4$ ,  $B_{yy} \approx -8.7$  and  $B_{zz} \approx 17.0 \text{ G}$ ) also show satisfactory agreement with the experimental values (see Table 1). The large angle between the CNO plane and the N—O $^\cdot$  bond ( $\varphi \approx 43^\circ$ ) and the slight differences between bond lengths found in DFT calculations appear to be due to specific features of one substituent (=Si—O—) at the N atom. Therefore, we believe that the conformation and the calculated geometric parameters of the

**Table 3.** Calculated and experimental HFC constants

| Atom | A/G                      |                         |                 |
|------|--------------------------|-------------------------|-----------------|
|      | Calculation <sup>a</sup> | Experiment <sup>b</sup> |                 |
|      |                          | I <sup>c</sup>          | II <sup>d</sup> |
| N    | 29.9                     | 31.6 (32.0)             | 31.2 (31.6)     |
| H(1) | 19.6                     | 17.7 (2.6)              | 7.2 (~1.1)      |
| H(2) | 0.7                      | 4.0                     | 7.2 (~1.1)      |
| H(3) | 0.5                      | -2.4                    | 7.2 (~1.1)      |

<sup>a</sup> Found by DFT calculations for the  $F_3SiON(O^\cdot)Me$  radical.

<sup>b</sup> Experimental HFC constants were determined with an accuracy of  $\pm 0.1 \text{ G}$ ; the values in parentheses are the constants for the  $=SiON(O^\cdot)CD_3$  radical.

<sup>c</sup> Determined from the data on the rigid limit simulation of the experimental spectra as  $A_{\text{iso}} = (A_{xx} + A_{yy} + A_{zz})/3$ .

<sup>d</sup> Found from the experimental spectrum at 298 K; H(1), H(2), and H(3) are equivalent.

$F_3SiON(O^\cdot)Me$  radical can be used to analyze experimental data of the grafted  $=SiON(O^\cdot)Me$  radical.

In grafted radicals, the isotropic constant of HFC with the N atom ( $A_{\text{iso}} \approx 31.2 \text{ G}$ ) is greater than the corresponding value in common nitroxides (14–16 G). This can be explained either by assuming that the  $>N—O^\cdot$  fragment in the obtained radical is essentially nonplanar, which should entail an increase in the spin density of the unpaired electron in the s-state and, correspondingly, an increase in the  $A_{\text{iso}}(N)$  value, or by assuming an increase in the spin-polarization constant caused by the presence of the second O atom in the  $>N—O^\cdot$  radical fragment. In our opinion, both factors are effective, but the latter appears to predominate. This assumption is supported by the following facts. On the one hand, for some nitroxides whose  $>N—O^\cdot$  fragments are pyramidal and the angles between the CNC plane and the N—O $^\cdot$  bond are 15–20°, the  $A_{\text{iso}}(N)$  values are known<sup>1</sup> to increase upon distortion of the planar geometry, but their values do not exceed 20 G. On the other hand, the  $A_{\text{iso}}(N)$  value for the  $MeON(O^\cdot)CMe_3$  radical having a similar structure is 29.5 G,<sup>18</sup> which virtually coincides with the corresponding value for the grafted radical.

**Rotational mobility of grafted radicals.** When analyzing data on the rotational mobility, it is necessary to define the system of coordinates of the  $\mathbf{g}$ -tensor in the grafted radical. It was found from experimental results for nitroxides<sup>1,3–5</sup> that the main axes of the  $\mathbf{g}$ -tensor have the same orientation with respect to the molecular axes of the radicals, namely, the  $x$  axis is directed along the N—O $^\cdot$  bond and the  $z$  axis coincides with the axis of the  $\pi$ -orbital of the unpaired electron; hence, the  $y$  axis is located approximately in the CNO $^\cdot$  plane because the deflection of the N—O $^\cdot$  bond from the CNC plane does not exceed ~20°. This orientation of the main axes of the  $\mathbf{g}$ -tensor is typical of radicals with similar properties of N-substituents in the paramagnetic fragment (as a rule, these are alkyl groups) in which the unpaired spin density is concentrated almost entirely on the N and O atoms. According to calculations,<sup>7</sup> a substantial portion of the density of the unpaired electron (~0.8) in grafted nitroxides is also concentrated in the p orbitals of the N and O atoms of the N—O $^\cdot$  fragment. The unpaired electron can interact with the lone electrons in the p orbitals of the two O atoms. Thus, one of the principal axes of the  $\mathbf{g}$ -tensor ( $z$  component) may be directed parallel to these orbitals and normal to the ONO $^\cdot$  plane. Thus the Cartesian xyz system in which the  $x$  axis is directed along the N—O $^\cdot$  bond, the  $y$  axis is located in the ONO $^\cdot$  plane, and the  $z$  axis is directed along the p orbital of the unpaired electron can be taken as the system of coordinates for the  $\mathbf{g}$ -tensor.

The experimental ESR spectra were simulated in terms of various motion models, namely, librations (small-amplitude high-frequency motions of a species in some potential field created by the environment; for disordered matrices, these are characterized by corre-

tion times of  $<10^{-9}$  s and angular amplitudes of  $\leq 5^\circ$ ),<sup>19</sup> Brownian diffusion, and MOMD (microscopic order—macroscopic disorder). In terms of the libration model, the amplitudes of librations around all the three axes were varied; however, this did not provide satisfactory description of the experimental spectra.

The anisotropic Brownian diffusion model in which the principal axes of magnetic parameters (**g**-tensor) coincided with the principal axes of the diffusion coefficient tensor (**R**-tensor) and the principal values of the **R**-tensor were varied also proved unsatisfactory for describing the motion of grafted radicals because the tensor components obtained by simulation changed arbitrarily upon temperature variation. A satisfactory description of the spectrum at 120 K was obtained by taking into account the noncoincidence of the directions of the principal axes of the **g** and **R** tensors; in this case, the variable parameters included not only the principal values of the **R**-tensor but also the angles which relate the *XYZ* system of coordinates of the rotation axes to the *xyz* system of coordinates of the **g**-tensor of the radical (Fig. 2). Although we were still unable to attain good agreement between the maxima of the simulated and experimental spectra, the obtained optimal parameters of the model demonstrated that the radical rotates fairly rapidly only around the *Z* axis ( $R = 6.5 \cdot 10^7$  s $^{-1}$ ). The Euler angles found allow one to determine the direction of this rotation axis in the **g**-tensor system of coordinates. The angles between the rotation axis (*Z*) and the **g**-tensor axes (*x*, *y*, *z*) were found to be 50, 43, and 75°, respectively (the values are given without allowance for the positive directions of the coordinate axes, *i.e.*, only values of  $<90^\circ$  are given).

It follows from the known structure of the grafted radical that the direction of either the N—O bond or the Si—O bond can serve as the rotation axis. From the

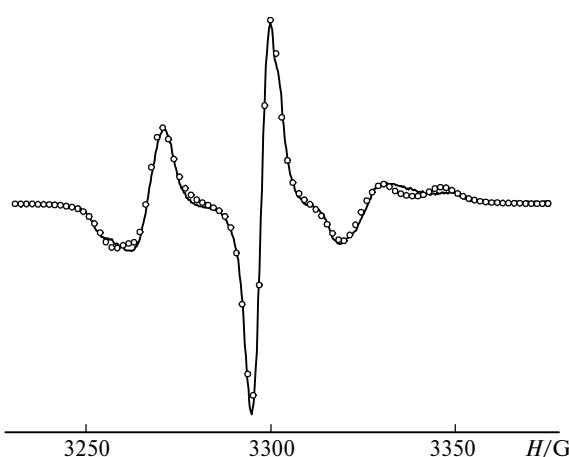


**Fig. 2.** Comparison of the experimental ESR spectrum of the  $\equiv\text{SiON}(\text{O}^\cdot)\text{CD}_3$  radicals at 120 K with the spectrum calculated with the assumption of the anisotropic Brownian diffusion with noncoinciding directions of the **g** and **R** tensors. The continuous line shows experimental spectrum and the dots correspond to calculations.

optimal geometry of the radical found by the DFT method, one can conclude that only with the assumption that the rotation axis is directed along the Si—O bond, are the angles between the rotation axis and *x*-, *y*-, and *z*-axes of the **g**-tensor calculated on the basis of the optimal geometry of the radical (70, 41, and 56°, respectively) close to those found by simulation of the experimental ESR spectrum; the agreement is improved as the Si—O—N—O<sup>·</sup> dihedral angle decreases. Thus, the maximum component of the **R**-tensor ( $R_z$ -component) is, apparently, directed normal to the plane through the three O atoms of the cluster linked directly to the Si atom, *i.e.*, it is directed approximately along the Si—O bond in the Si—O—N fragment (according to calculations, the angle between the normal and the direction of the Si—O bond in the energetically optimal conformation of the radical amounts to  $\sim 7^\circ$ ). This conclusion is consistent with experimental data on the barriers to the rotation of molecular<sup>17</sup> or radical<sup>20–22</sup> fragments around the Si—O bond ( $\leq 3$  kcal mol $^{-1}$ ). According to calculations for the  $\equiv\text{SiON}(\text{O}^\cdot)\text{Me}$  radical (Table 4), of the two possible types of fragment rotations that can result in averaging of the anisotropic HFC with the N nucleus and the anisotropic Zeeman interaction of the radical (around the Si—O and N—O bonds), the barrier to rotation around the Si—O bond is less significant.

Thus, analysis of the structural and dynamic data allowed the assignment of the principal values of the **g**-tensor (see Table 1) and identification of the axis corresponding to the least hindered rotation.

The anisotropic Brownian diffusion model and the MOMD model were also used to perform quantitative simulation of the experimental spectrum recorded at  $\sim 180$  K, *i.e.*, for simulation of the spectrum of radicals possessing rather high mobility. The values of potentials whose presence is responsible for the rotation anisotropy were varied within the framework of this model. It can be seen that the MOMD model provides a more adequate description of the experimental spectrum (Fig. 3). The height of the potential barrier to the

**Table 4.** Barriers to the rotation ( $\Delta E$ ) of radical fragments around various bonds

| Bond                   | $\Delta E/\text{kcal mol}^{-1}$ |                 |
|------------------------|---------------------------------|-----------------|
|                        | I <sup>a</sup>                  | II <sup>b</sup> |
| O—N(O <sup>·</sup> )Me | 4.6                             | 5.4             |
| Si—O                   | 3.4                             | 2.7             |
| N(O <sup>·</sup> )—Me  | 1.8                             | 1.7–1.8         |

<sup>a</sup> Found by DFT calculations for the  $\text{F}_3\text{SiON}(\text{O}^\cdot)\text{Me}$  radical.

<sup>b</sup> Estimated from the experimental data for the grafted  $\equiv\text{SiON}(\text{O}^\cdot)\text{Me}$  or  $\equiv\text{SiON}(\text{O}^\cdot)\text{CD}_3$  radical.

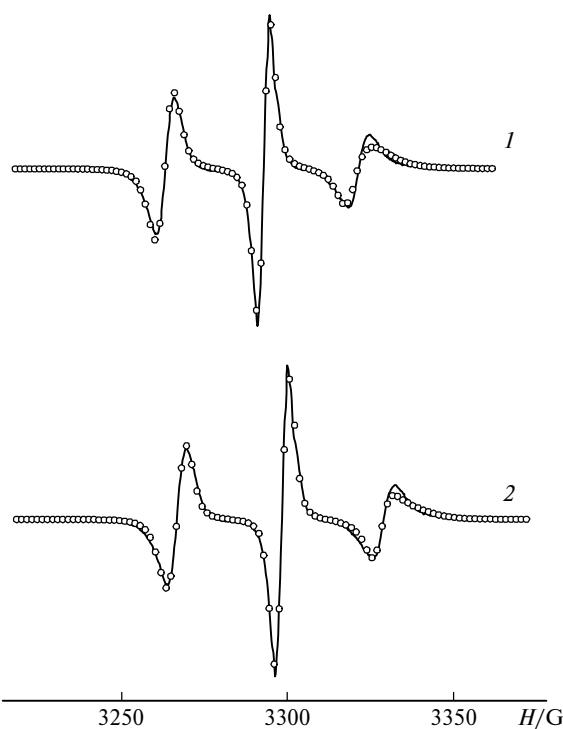


**Fig. 3.** Results of the simulation of the ESR spectra of the  $\equiv\text{SiON}(\text{O}\cdot)\text{CD}_3$  radicals at 180 K in terms of the anisotropic Brownian diffusion (1) and MOMD (2) models. The continuous lines show experimental spectra and the dots correspond to calculations.

rotation around the principal axis was found to be  $\sim 2$  kcal mol $^{-1}$ .

**Estimation of the rotation barriers of radical fragments around various bonds.** We studied the ESR spectra of the grafted  $\equiv\text{SiON}(\text{O}\cdot)\text{Me}$  radicals recorded at temperatures above 77 K (see Fig. 1, a). The change in the spectral pattern at 110–120 K (the appearance of a clear-cut quartet of lines in the central part of the spectrum, see Fig. 1, a, curve 2) attests to the averaging of the anisotropic HFC constants of protons. Hence, at this temperature, the methyl group of the grafted radical starts to rotate (or execute large-amplitude oscillations) around the C–N bond, the frequency of this motion being sufficient for averaging of the anisotropic part of the HFC with the methyl-group proton. Since the anisotropic component at the methyl-group protons equals  $\sim 10$ –15 G (see Table 1), the  $v_{\text{aniso}} \approx (10\text{--}15) \cdot 2.8 \cdot 10^6 \approx (3\text{--}4) \cdot 10^7$  s $^{-1}$ , where  $2.8 \cdot 10^6$  s $^{-1}$  G $^{-1}$  is the gyromagnetic ratio for an electron. Taking the pre-exponential factor in the rotation of the methyl group to be  $10^{12}$  s $^{-1}$ , one can estimate the activation energy for the rotation of the methyl group in the grafted radical to be  $\Delta E \approx 1.7\text{--}1.8$  kcal mol $^{-1}$ .

Study of the spectra of the  $\equiv\text{SiON}(\text{O}\cdot)\text{CD}_3$  radicals recorded at temperatures above 77 K (see Fig. 1, b) showed that at  $\sim 120$  K, the symmetry of the Zeeman interaction tensor becomes axial, while at  $\sim 300$  K, the

Zeeman interaction tensor is virtually isotropic (the heights of the low-field and high-field components are almost equal, see Fig. 1, curve 4). It can be assumed with high probability that the axial symmetry of the **g**-tensor is achieved as a result of rotation of the grafted radical around the Si–O bond due to averaging of the  $g_{xx}$ - and  $g_{yy}$ -components, while the isotropy of the **g**-tensor is a result of rotation of radical fragments around the Si–O and N–O bonds simultaneously.

The activation energies for the rotation around the Si–O bond ( $g \approx 2.005$ ,  $\Delta g \approx 0.001$  and  $T \approx 110$  K) and around the N–O bond ( $g \approx 2.005$ ,  $\Delta g \approx 0.004$  and  $T \approx 300$  K) were found by a similar scheme with allowance for the relation  $v_{\text{aniso}} \approx v_0(g_{xx} - g_{yy})/g$ . This gave 2.7 and 5.4 kcal mol $^{-1}$ , respectively. The resulting values are in satisfactory agreement with the heights of the activation barriers to the rotation of radical fragments around various bonds calculated by the DFT method (see Table 4) and with the height of the barrier to the rotation of the radical around the Si–O bond determined from analysis of the rotational mobility in terms of the MOMD model ( $\sim 2$  kcal mol $^{-1}$ ).

Thus, we determined the principal values of the **g**-tensor and the HFC tensors of magnetic nuclei (N, H) for the grafted  $\equiv\text{SiON}(\text{O}\cdot)\text{CX}_3$  radicals ( $X = \text{H}, \text{D}$ ) and assigned the principal values of the **g**-tensor to molecular axes of the radical. The barriers to the rotation of radical fragments around various bonds were estimated. The radical mobility was characterized by the rotational diffusion tensor.

This work was supported by the Russian Foundation for Basic Research (Project No. 00-03-32109) and the scientific program "Russian Universities — Fundamental Research" (Project No. 990399).

## References

1. A. L. Buchachenko and A. M. Vasserman, *Stabil'nye radikaly [Stable Radicals]*, Khimiya, Moscow, 1973, 408 pp. (in Russian).
2. A. L. Buchachenko, *Kompleksy radikalov i molekulyarnogo kisloroda s organiceskimi molekulami [Complexes of Radicals and Dioxygen with Organic Molecules]*, Nauka, Moscow, 1984, 157 pp. (in Russian).
3. A. N. Kuznetsov, *Metod spinovogo zonda (osnovy i primenenie) [Spin Probe Method. Foundations and Applications]*, Nauka, Moscow, 1976, 210 pp. (in Russian).
4. *Spin Labelling, Theory and Applications*, Ed. L. J. Berliner, Academic Press, New York—San Francisco—London, 1976.
5. L. B. Volodarskii, I. A. Grigor'ev, S. A. Dikanov, V. A. Reznikov, and G. I. Shchukin, *Imidazolinovye nitroksil'nye radikaly [Imidazoline Nitroxides]*, Nauka, Sib. otd-nie, Novosibirsk, 1988, 216 pp. (in Russian).
6. V. B. Golubev, E. V. Lunina, and A. K. Selivanovskii, *Usp. Khim.*, 1981, **50**, 792 [*Russ. Chim. Rev.*, 1981, **50** (Engl. Transl.)].
7. V. I. Pergushov, N. Yu. Osokina, P. I. Naumenko, and M. Ya. Mel'nikov, *Dokl. Akad. Nauk*, 2001, **376**, 66 [*Dokl. Chem.*, 2001 (Engl. Transl.)].

8. V. A. Radtsig, *Khim. Fizika*, 1991, **10**, 1262 [*Chem. Phys.*, 1991, **10** (Engl. Transl.)].
9. V. A. Gritsenko, A. A. Milov, and H. Wong, *Modern Applications of EPR/ESR from Biophysics to Material Science, Proc. of the 1st Asia-Pacific EPR/ESR Symp. (Hong Kong)*, Ed. C. Z. Rudowicz, Springer, Berlin, 1997, 613.
10. D. J. Schneider and J. Freed, *Calculating Slow Motion Magnetic Resonance Spectra: a User's Guide in Biological Magnetic Resonance*, (Eds. L. J. Berliner and J. Reuben), Plenum, New York, 1989, **8**.
11. J. E. Dennis, D. M. Gay, and R. E. Welsch, *Transactions Mathematical Software*, 1981, **7**, 348; 369.
12. A. Kh. Vorob'ev, V. S. Gurman, and T. A. Klimenko, *Izv. Akad. Nauk, Ser. Khim.*, 2000, 1065 [*Russ. Chem. Bull., Int. Ed.*, 2000, **49**, 1059].
13. D. N. Laikov, *Chem. Phys. Lett.*, 1997, **281**, 151.
14. M. A. Ondar, O. Ya. Grinberg, A. A. Dubinskii, A. F. Shestakov, and Ya. S. Lebedev, *Khim. fizika*, 1983, **2**, 54 [*Chem. Phys.*, 1983, **2** (Engl. Transl.)].
15. V. A. Radtsig, and I. N. Senchenya, *Khim. fizika*, 1991, **10**, 322 [*Chem. Phys.*, 1991, **10** (Engl. Transl.)].
16. B. Anderson and P. Anderson, *Acta Chem. Scand.*, 1966, **20**, 2728.
17. M. G. Voronkov, V. P. Mileshkevich, and Yu. A. Yuzhelevskii, *Siloksanovaya svyaz'* [Siloxane Bond], Nauka, Novosibirsk, 1976, 410 pp. (in Russian).
18. V. E. Zubarev, V. N. Belevskii, and L. T. Bugaenko, *Khimiya Vysok. Energii*, 1977, **11**, 91 [*High Energy Chem.*, 1977, **11** (Engl. Transl.)].
19. S. V. Paschenko, S. A. Dzuba, A. Kh. Vorobiev, Yu. V. Toropov, and Yu. D. Tsvetkov, *J. Chem. Phys.*, 1999, **110**, 8150.
20. V. I. Pergushov, E. G. Evtikhieva, and D. A. Tyurin, *Izv. Akad. Nauk, Ser. Khim.*, 1999, 2092 [*Russ. Chem. Bull.*, 1999, **48**, 2069 (Engl. Transl.)].
21. V. I. Pergushov and M. K. Kuimova, *Izv. Akad. Nauk, Ser. Khim.*, 2000, 1862 [*Russ. Chem. Bull., Int. Ed.*, 2000, **49**, 1834 (Engl. Transl.)].
22. V. I. Pergushov, *Zh. Fiz. Khim.*, 2001, **75**, 860 [*Russ. J. Phys. Chem.*, 2001, **75** (Engl. Transl.)].

Received July 20, 2001;  
in revised form August 6, 2001